The contribution of cloud and radiation anomalies to the 2007 Arctic sea ice extent minimum

Jennifer E. Kay,[1,2] Tristan L'Ecuyer,[2] Andrew Gettelman,[1] Graeme Stephens,[2] and Chris O'Dell[2]

Received 29 January 2008; revised 7 March 2008; accepted 13 March 2008; published 22 April 2008.

[1] Reduced cloudiness and enhanced downwelling radiation are associated with the unprecedented 2007 Arctic sea ice loss. Over the Western Arctic Ocean, total summertime cloud cover estimated from spaceborne radar and lidar data decreased by 16% from 2006 to 2007. The clearer skies led to downwelling shortwave (longwave) radiative fluxes increases of +32 Wm^{-2} (−4 Wm^{-2}) from 2006 to 2007. Over three months, simple calculations show that these radiation differences alone could enhance surface ice melt by 0.3 m, or warm the surface ocean by 2.4 K, which enhances basal ice melt. Increased air temperatures and decreased relative humidity associated with an anti-cyclonic atmospheric circulation pattern explain the reduced cloudiness. Longer-term observations show that the 2007 cloudiness is anomalous in the recent past, but is not unprecedented. Thus, in a warmer world with thinner ice, natural summertime circulation and cloud variability is an increasingly important control on sea ice extent minima.
Citation: Kay, J. E., T. L'Ecuyer, A. Gettelman, G. Stephens, and C. O'Dell (2008), The contribution of cloud and radiation anomalies to the 2007 Arctic sea ice extent minimum, *Geophys. Res. Lett.*, *35*, L08503, doi:10.1029/2008GL033451.

1. Introduction

[2] Passive microwave satellite observations, available from 1979 to present, show declines in Arctic sea ice extent. Downward trends, while present in all months, are largest in September when the ice reaches its annual minimum extent. While the downward trend in the minimum ice extent has substantial inter-annual variability, the 2007 minimum extent represents a dramatic departure from the historical trend line [*Stroeve et al.*, 2008]. The 2007 minimum extent was 4.13 million km^2 on September 16, 2007, down 43% from 1979 and down 22% from the previous record in 2005. During 2007, large negative anomalies in ice extent persisted from July through early September, mostly in the Pacific sector of the Arctic.

[3] Multiple factors conspired to produce the observed sea ice loss, but their relative importance remains unknown. Contributing factors identified before summer 2007 include: the decline of thick perennial sea ice [*Nghiem et al.*, 2007; *Maslanik et al.*, 2007], wind-induced changes in sea ice distribution associated with cyclonic wintertime circulation patterns [*Rigor and Wallace*, 2004] and anti-cyclonic summertime circulation patterns [*Ogi and Wallace*, 2007], enhanced heat transport to the Arctic by the ocean [*Shimada et al.*, 2006] and the atmosphere [*Serreze et al.*, 2007], and enhanced absorption of solar radiation by the ocean associated with sea ice extent reductions [*Perovich et al.*, 2007].

[4] Here, we demonstrate that reduced cloudiness and enhanced downwelling shortwave radiation contributed to the record 2007 sea ice extent loss. Based on our findings, we suggest that in a warmer Arctic with thinner ice, cloud and shortwave radiation anomalies will play an increasingly important role in modulating summertime sea ice extent.

2. Methods

[5] Remote sensing instruments on NASA's A-train satellite platforms are uniquely capable of measuring Arctic clouds and constraining radiative flux calculations. With data available from June 15, 2006 to present, CloudSat's 94-GHz cloud profiling radar (CPR) [*Stephens et al.*, 2002] and CALIPSO (Cloud-Aerosol Lidar and Infrared Pathfinder Satellite Observation)'s 532-nm and 1064-nm Cloud-Aerosol Lidar with Orthogonal Polarization (CALIOP) lidar provide the first capability to document the vertical structure of Arctic clouds. Combined radar-lidar cloud masks from CloudSat standard products (2B-GEOPROF and 2B-GEOPROF-LIDAR) provide a highly accurate measurement of cloud fraction profiles. Unlike cloud detection techniques based on passive radiances, combined radar-lidar cloud detection does not rely on the weak thermal and albedo contrast between clouds and the often ice-covered Arctic surface. Instead, cloud detection relies on the amount of energy backscattered by cloud particles. The only clouds that combined CloudSat-CALIOP data cannot identify are in the bottom 720 m of the atmosphere when surface clutter contaminates the radar backscatter and the lidar backscatter is attenuated by absorption due to a thick overlying cloud.

[6] To quantify the impact of Arctic clouds on the surface radiation budget, we estimate surface downwelling shortwave and longwave radiation using an enhanced version of the CloudSat fluxes and heating rates product (2B-FLXHR). A detailed description of the standard 2B-FLXHR radiative transfer algorithm is available in the 2B-FLXHR Theoretical Basis Document (available at http://cloudsat.cira.colostate.edu). The algorithm constrains radiative flux profiles using liquid and ice cloud microphysical property information from CloudSat's 2B-CWC product, and ancillary atmospheric and surface property datasets. Because the standard 2B-FLXHR product only incorporates CloudSat clouds, we modified the algorithm to add clouds exclusively observed by CALIOP. CALIOP-only low clouds, which CloudSat misses due to

[1]Climate and Global Dynamics Division, National Center for Atmospheric Research, Boulder, Colorado, USA.
[2]Department of Atmospheric Sciences, Colorado State University, Fort Collins, Colorado, USA.

0094-8276/08/2008GL033451$05.00

Table 1. Western Arctic (120–180 W, 70 N +) Melt Season Cloud Fraction[a]

Melt Year	MODIS Terra[b] JJA (JJ)	MODIS Aqua[b] JJA (JJ)	CloudSat[b] jJJs	CloudSat and CALIOP[c] jJJs	CloudSat and CALIOP[c] jJJs Low	Barrow Ceilometer JJA
1998	-	-	-	-	-	0.79
1999	-	-	-	-	-	0.74
2000	0.58 (0.54)	-	-	-	-	0.80
2001	0.67 (0.65)	-	-	-	-	0.81
2002	0.63 (0.57)	-	-	-	-	0.79
2003	0.69 (0.63)	0.70 (0.64)	-	-	-	0.82
2004	0.60 (0.52)	0.61 (0.53)	-	-	-	0.76
2005	0.53 (0.46)	0.55 (0.47)	-	-	-	0.74
2006	0.60 (0.58)	0.62 (0.58)	0.57	0.78	0.63	0.78
2007	0.46 (0.40)	0.48 (0.42)	0.39	0.61	0.51	0.63
2007–2006 Difference	−0.14 (−0.17)	−0.13 (−0.17)	−0.18	−0.16	−0.12	−0.15
2007 Percent Anomaly	−23% (−26%)	−18% (−21%)	-	-	-	−18%

[a]For clarity, we report cloudiness as a fraction, while percent anomalies in cloudiness are reported as a percentage.
[b]MODIS cloud fractions are daytime averages from June 1 to August 31 (JJA), and from June 1 to July 31 (JJ). They are calculated from the Cloud_Fraction_Combined Level-3, collection 5 product [see *Platnick et al.*, 2003].
[c]CloudSat/CALIOP cloud fractions are found on a profile-by-profile basis from June 15 to September 15 (jJJs). Positive cloud ID required a cloud thickness of 960 m (480 m for low clouds). Low clouds occur below 2.75 km. CloudSat data in the 720 m are excluded due to surface clutter. Based on evaluating the influence of cloud definition and data quality flag interpretation on our radar-lidar analysis, we estimate that errors in the 2007–2006 cloud fraction difference are less than 0.02. The combined CloudSat/CALIOP statistics exclude 28 days in 2006, and 17 days in 2007 due to lidar data quality concerns.

surface clutter, are assumed to have a liquid water path (LWP) of 0.05 g m^{-3} and an effective radius of 9 μm, consistent with ground-based observations [*Curry et al.*, 2000]. CALIOP-only high clouds, which CloudSat misses because they are optically thin, are assumed to have an ice water path (IWP) of 0.004 g m^{-3} and an effective radius of 30 μm, consistent with extinction observations from a high spectral resolution lidar operated in Eureka, Canada (http://www.candac.ca).

[7] In addition to the CloudSat/CALIOP observations, we analyze Moderate Resolution Imaging Spectroradiometer (MODIS) radiance-based estimates of Arctic cloudiness [*Platnick et al.*, 2003]. Two MODIS datasets are available: MODIS Terra and MODIS Aqua. In addition to providing temporal context for the short CloudSat/CALIOP record, MODIS has better spatial sampling than CloudSat/CALIOP and can be used to evaluate the timing of cloud fraction changes.

[8] To quantify atmospheric temperature and humidity profiles, we use retrievals based on V4 Atmospheric Infrared Sounder (AIRS) data [*Gettelman et al.*, 2006]. AIRS, which is on the same satellite platform as MODIS, is a scanning nadir infrared sounder. *Gettelman et al.* [2006] showed that AIRS retrievals in polar regions are unbiased relative to in-situ radiosondes.

[9] To validate, extend, and provide historical context for the satellite cloud and radiation records, we analyze ground-based observations from Barrow, Alaska (71.3 N, 156.6 W) and the National Centers for Environmental Prediction (NCEP) reanalysis [*Kalnay et al.*, 1996]. We assess historical cloud cover using sixty-two years (1946–2007) of surface observations from the Integrated Surface Hourly (ISH) database compiled by the NOAA/National Climatic Data Center. We estimate cloud fraction on a daily basis by assuming "overcast" is equivalent to cloud fraction = 1, "broken cloud" is equivalent to cloud fraction = 0.75, "scattered" is equivalent to cloud fraction = 0.31, and "clear" is equivalent to cloud fraction = 0. We also analyze ten years (1998–2007) of cloud and radiation observations from the Atmospheric Radiation Measurement (ARM) North Slope of Alaska (NSA) site at Barrow [*Stamnes et al.*, 1999]. The upward-looking ceilometer data are used to estimate cloud cover, while radiative fluxes are found using a pyranometer for downwelling shortwave radiation and a shaded pyrgeometer for downwelling longwave radiation.

3. Results

[10] CloudSat, CALIOP, and MODIS data all reveal dramatic decreases in cloudiness over the Western Arctic Ocean (120 to 180 W, 70 to 90 N) during summer 2007 (Table 1). The combined radar-lidar total cloud fraction decreased by 0.16 from 0.78 (2006) to 0.61 (2007). As a result of differences in temporal and spatial sampling, and cloud detection techniques, the percent anomalies in 2007 summertime cloudiness over the recent past ranged from −18% to −26%. MODIS cloud fraction data indicated that cloud anomalies were largest in June and July, coincident with the peak in solar insolation.

[11] Reductions in CloudSat and CALIOP cloud fractions over the Western Arctic occurred at all heights, especially poleward of 70 N (Figures 1a–1d). Adding the lidar data to the radar-only cloud fraction profiles did not result in an appreciable change to the inferred vertical distribution of clouds. AIRS retrievals show that 2 to 4 K temperature increases and 0 to 10% relative humidity decreases in the same region as the cloudiness decreases (Figures 1e–1f). The AIRS retrievals also show small increases in specific humidity (not shown) demonstrating temperature increases outpaced moisture increases.

[12] Associated with the 2007–2006 cloud decreases, estimated net downwelling radiation in the Western Arctic Ocean increased by 28 Wm^{-2} (Figure 2). Downwelling shortwave radiation increased by 32 Wm^{-2} from 171 Wm^{-2} (2006) to 204 Wm^{-2} (2007), while downwelling longwave radiation decreased by 4 Wm^{-2} from 289 Wm^{-2} (2006) to 285 Wm^{-2} (2007). Based on ongoing evaluation of the 2B-FLXHR product using independent flux estimates from Clouds and the Earth's Radiant Energy System (CERES), the uncertainties in downwelling shortwave and longwave radiation are approximately 11 and 8 Wm^{-2} respectively.

[13] Simple calculations reveal the importance of the observed cloud and radiation differences for sea ice melt

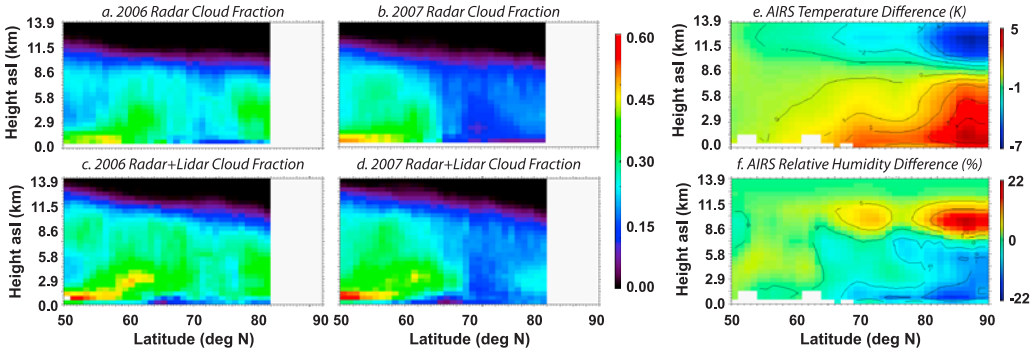

Figure 1. Zonal mean profiles in the Western Arctic (−120 to −180 E) during the summer melt season: (a)–(d) June 15–Sept. 15 cloud fraction profiles from 2006 and 2007 and (e)–(f) June 15–Sept 7 AIRS-derived temperature and relative humidity profile differences (2007–2006).

and heating of the surface ocean. If sustained over a 3-month period over an ice-covered ocean, the 2007 minus 2006 downwelling flux differences derived from the enhanced 2B-FLXHR algorithm could enhance surface melt by 0.3 m:

$$\Delta I = \frac{[(\Delta RF_{sw}*(1-a_{ice}))+\Delta RF_{lw}]*t}{L_{fusion}*\rho_{ice}} \quad (1)$$

where ΔI is the additional depth of surface ice melted (m), ΔRF_{sw} is the change in the shortwave downwelling irradiance (W m^{-2}), ΔRF_{lw} is the change in the longwave downwelling irradiance (W m^{-2}), $a_{ice} = 0.5$ is a reasonable average albedo of the ice surface over the melt season [*Curry et al.*, 2000], t = 3 months (seconds), L_{fusion} = 334000 is the latent heat of fusion (J kg^{-1}), and $\rho_{ice} = 917$ is the density of ice (kg m^{-3}).

[14] After the sea ice melts, the surface ocean can absorb a large fraction of the downwelling radiation [e.g., *Perovich et al.*, 2007]. If sustained over a 3-month period over an open ocean, the observed changes in downwelling radiation could increase ocean mixed layer temperatures by 2.4 K:

$$\Delta T = \frac{[(\Delta RF_{SW}*(1-a_{ocean}))+\Delta RF_{lw}]*t}{C^*_{ocean}\rho^*_{ocean}D} \quad (2)$$

where ΔT is increase in the ocean mixed layer temperature (K), $a_{ocean} = 0.07$ is the ocean surface albedo [*Perovich et al.*, 2007], $C_{ocean} = 4186$ is the specific heat of ocean water (J kg^{-1} K^{-1}), $\rho_{ocean} = 1030$ is the density of sea water (kg m^{-3}), and D = 20 m is an estimate of the average depth of the summertime ocean mixed layer in the Western Arctic [*Monterey and Levitus*, 1997]. If one assumes that all of the additional heat absorbed by the ocean is used to melt sea ice in a marginal ice zone with 50% ice cover and 50% ocean cover, a simple calculation following equation (1) suggests basal melting could be enhanced by 0.7 m.

[15] While these rough calculations mask large variability in both time and space (e.g., sea ice albedo variability associated with melt ponds and snow cover, variability in the mixed layer depth) and the complexity of the processes that result in melt at the sea ice margin [e.g., *Bitz et al.*, 2005], they do indicate a significant potential for the 2007 minus 2006 radiation differences to reduce sea ice extent and thickness. According to ice-tracking algorithms [*Maslanik et al.*, 2007] and ICESat satellite retrievals [*Stroeve et al.*, 2008], March sea ice thicknesses in the Western Arctic in 2007 were <1.5 m. Thus, an additional 0.3 m of surface melt or 0.7 m of basal melt represents a significant fraction of the ice thickness at the beginning of the melt season.

[16] Surface observations from Barrow, Alaska (156.6 W, 71.3 N) provide historical context for the short satellite

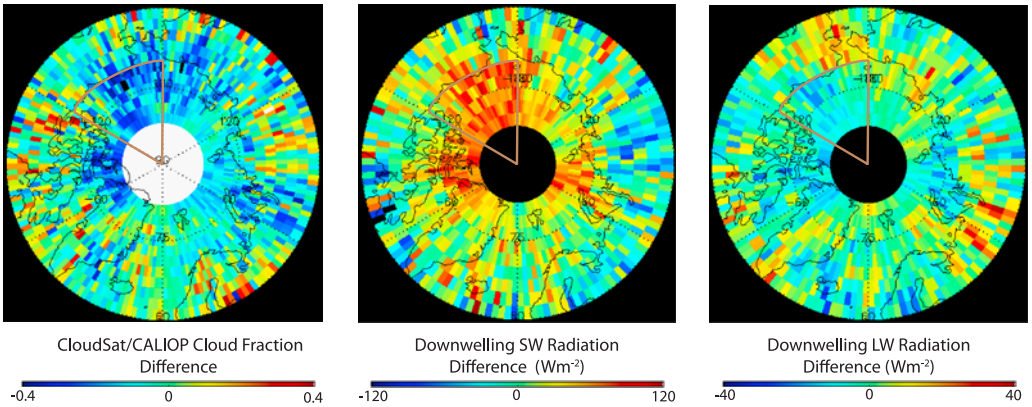

Figure 2. Clouds and downwelling radiation 2007–2006 differences (June 15–Sept 15). (left) Total cloud fraction differences based on radar and lidar data. (middle) Downwelling SW radiative flux difference. (right) Downwelling LW radiative flux difference. The Western Arctic Ocean is outlined in brown.

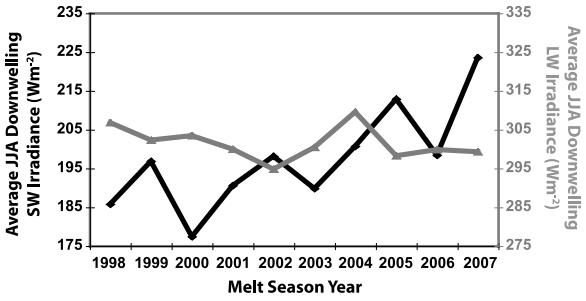

Figure 3. Ground-based radiation observations at Barrow, Alaska.

records. In the recent past, the ARM NSA data confirm the anomalous nature of the satellite-observed 2007 clouds and radiative fluxes. The JJA ceilometer-estimated cloud fraction was 0.63, which was the smallest cloud cover in the 1998-2007 record and 2.5 standard deviations below the mean cloudiness (Table 1). In addition, the average 2007 downwelling shortwave (longwave) radiation was 26 Wm^{-2} (-2 Wm^{-2}) greater than the 10-year mean (Figure 3). Despite differences in temporal and spatial sampling, the flux differences from the enhanced 2B-FLXHR algorithm and the Barrow observations are surprisingly consistent.

[17] Analysis of the 62-year Barrow ISH surface observations record reveals that the 2007 cloud conditions are not unprecedented. The JJA 2007 cloud fraction estimated from the ISH data was 0.77, a 0.06 decrease from the 1946-2007 mean, but not distinct from the mean at the 99% confidence level. In addition, five years (1991, 1977, 1976, 1971, 1968) had lower cloud cover than 2007.

[18] The observed thermodynamic forcing anomalies reflect the 2007 summertime atmospheric circulation pattern, which was characterized by persistent high sea level pressure (SLP) over the Western Arctic and low SLP over Siberia [*Stroeve et al.*, 2008] (Figure 4). The largest cloud reductions and shortwave radiation increases were co-located with the anticyclone center and were associated with subsidence. The largest temperature increases were centered over the date line and were associated with warm southerly winds.

4. Discussion

[19] The unprecedented 2007 sea ice extent confirms that an anti-cyclonic summertime atmospheric circulation pattern in the Western Arctic is a potent forcing for sea ice loss (Figure 4). *Ogi and Wallace* [2007] (OW07) recently identified summertime circulation anomalies as being an important control on sea ice extent minima. Although OW07 invoke anomalous wind stress associated with strong SLP gradients and its affect on ice transport as the mechanism to link anti-cyclonic patterns and ice extent, our analysis points to additional contributing mechanisms. First, in addition to modifying ice transport, southerly wind anomalies enhance poleward atmospheric heat transport (Figure 4). Second, warm and dry conditions associated with the anti-cyclonic circulation lead to reduced cloudiness and enhanced downwelling shortwave radiation. Solar flux increases lead to more melt at the ice surface, but perhaps more importantly, they heat the surface ocean and thus can indirectly enhance basal ice melt. These ice melt factors may have also conspired during 2005, when like 2007, a record sea ice extent minimum was associated with an anti-cyclonic circulation pattern (not shown) and reduced cloudiness (Table 1).

[20] This work also suggests that the relative importance of the downwelling shortwave and longwave radiation in controlling Arctic sea ice extent is changing. Except for short time periods in the summer, longwave radiation dominates the Arctic radiation budget because of the lack of sun, the large solar zenith angle, and the high surface albedo [*Curry et al.*, 1996]. As a result, decreases in Arctic cloud amounts are generally associated with decreases in downwelling radiation, and enhanced surface cooling. *Francis et al.* [2005] (F05) showed that downwelling longwave radiation explained 40% of the year-to-year minimum sea ice extent variations, while anomalies in downwelling shortwave radiation were actually negatively correlated with ice retreat. The F05 findings contradict what is found during 2005 and 2007, namely that reduced cloudiness and increased shortwave radiation are associated with sea ice extent minima. The F05 analysis did not examine recent years such as 2005 and 2007 in which positive shortwave radiation anomalies are associated with reduced sea ice extent. Decreases in the system albedo, i.e., the combined surface and cloud albedo, associated with sea ice decline are consistent with an increased role for shortwave radiation during the summer melt season.

5. Summary

[21] Satellite and ground-based observations show that decreased cloudiness and increased downwelling shortwave

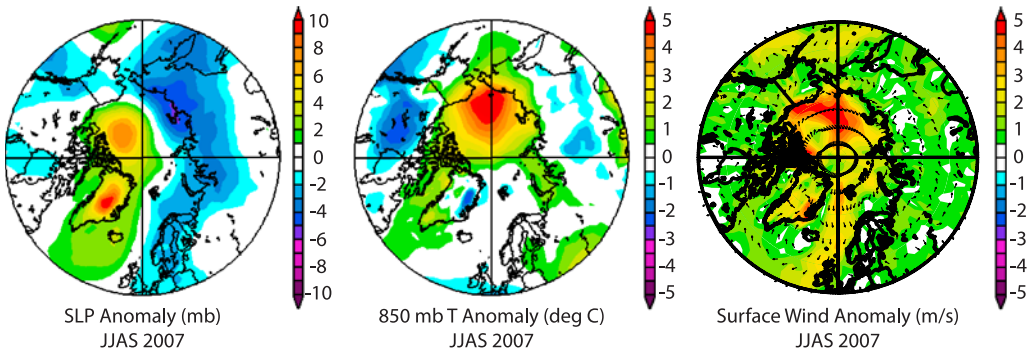

Figure 4. Sea level pressure (mb), 850 air temperature (deg C), and surface wind anomalies (m/s) from the NCEP reanalysis project.

radiation are associated with the record-breaking 2007 sea ice extent minimum. While the 2007 cloud reductions are anomalous in the recent past, a 62-year record of cloudiness from Barrow hints that the 2007 cloudiness was not unprecedented. Thus, our results suggest that when sea ice is vulnerably thin, natural year-to-year variations in the summertime atmospheric circulation and associated changes in clouds and shortwave radiation can play an increasingly large role in modulating sea ice extent.

[22] **Acknowledgments.** This work was funded by the NASA CloudSat project, with additional contributions from NSF, ARM DOE, and NEWS. JEK thanks Marika Holland and Clara Deser for helpful discussions.

References

Bitz, C. M., M. M. Holland, E. Hunke, and R. E. Moritz (2005), Maintenance of the sea-ice edge, *J. Clim.*, *18*, 2903–2921.

Curry, J. A., W. B. Rossow, D. Randall, and J. L. Schramm (1996), Overview of Arctic cloud and radiation characteristics, *J. Clim.*, *9*, 1731–1764.

Curry, J. A., et al. (2000), FIRE Arctic Clouds Experiment, *Bull. Am. Meteorol. Soc.*, *81*, 5–29.

Francis, J. A., E. Hunter, J. R. Key, and X. Wang (2005), Clues to variability in Arctic minimum sea ice extent, *Geophys. Res. Lett.*, *32*, L21501, doi:10.1029/2005GL024376.

Gettelman, A., V. P. Walden, L. M. Miloshevich, W. L. Roth, and B. Halter (2006), Relative humidity over Antarctica from radiosondes, satellites, and a general circulation model, *J. Geophys. Res.*, *111*, D09S13, doi:10.1029/2005JD006636.

Kalnay, E., et al. (1996), The NCEP/NCAR reanalysis 40-year project., *Bull. Am. Meteorol. Soc.*, *77*, 437–471.

Maslanik, J. A., C. Fowler, J. Stroeve, S. Drobot, J. Zwally, D. Yi, and W. Emery (2007), A younger, thinner Arctic ice cover: Increased potential for rapid, extensive sea-ice loss, *Geophys. Res. Lett.*, *34*, L24501, doi:10.1029/2007GL032043.

Monterey, G. I., and S. Levitus (1997), Climatological cycle of mixed layer depth in the world ocean, 5 pp., U.S. Gov. Print. Off., Washington, D. C.

Nghiem, S. V., I. G. Rigor, D. K. Perovich, P. Clemente-Colón, J. W. Weatherly, and G. Neumann (2007), Rapid reduction of Arctic perennial sea ice, *Geophys. Res. Lett.*, *34*, L19504, doi:10.1029/2007GL031138.

Ogi, M., and J. M. Wallace (2007), Summer minimum Arctic sea ice extent and the associated summer atmospheric circulation, *Geophys. Res. Lett.*, *34*, L12705, doi:10.1029/2007GL029897.

Perovich, D. K., B. Light, H. Eicken, K. F. Jones, K. Runciman, and S. V. Nghiem (2007), Increasing solar heating of the Arctic Ocean and adjacent seas, 1979–2005: Attribution and role in the ice-albedo feedback, *Geophys. Res. Lett.*, *34*, L19505, doi:10.1029/2007GL031480.

Platnick, S., M. D. King, S. A. Ackerman, W. P. Menzel, B. A. Baum, J. C. Riedi, and R. A. Frey (2003), The MODIS cloud products: Algorithms and examples from Terra, *IEEE Trans. Geosci. Remote Sens.*, *41*, 459–473.

Rigor, I. G., and J. M. Wallace (2004), Variations in the age of Arctic sea-ice and summer sea-ice extent, *Geophys. Res. Lett.*, *31*, L09401, doi:10.1029/2004GL019492.

Serreze, M. C., M. M. Holland, and J. Stroeve (2007), Perspectives on the Arctic's shrinking sea-ice cover, *Science*, *315*, 1533–1536, doi:10.1126/science.1139426.

Shimada, K., T. Kamoshida, M. Itoh, S. Nishino, E. Carmack, F. A. McLaughlin, S. Zimmermann, and A. Proshutinsky (2006), Pacific Ocean inflow: Influence on catastrophic reduction of sea ice cover in the Arctic Ocean, *Geophys. Res. Lett.*, *33*, L08605, doi:10.1029/2005GL025624.

Stamnes, K., R. G. Ellingson, J. A. Curry, J. E. Walsh, and B. D. Zak (1999), Review of science issues, deployment strategy, and status for the ARM North Slope of Alaska-Adjacent Arctic Ocean climate research site, *J. Clim.*, *12*, 46–63.

Stephens, G. L., et al. (2002), The CloudSat mission and the A-Train: A new dimension of spacebased observations of clouds and precipitation, *Bull. Am. Meteorol. Soc.*, *83*, 1771–1790.

Stroeve, J., M. Serezze, S. Drobot, S. Gearheard, M. Holland, J. Maslanik, W. Meier, and T. Scambos (2008), Arctic sea ice plummets in 2007, *Eos Trans. AGU*, *89*, 13.

T. L'Ecuyer, C. O'Dell, and G. Stephens, Department of Atmospheric Sciences, Colorado State University, Fort Collins, CO 80523-1371, USA.

A. Gettelman and J. E. Kay, Climate and Global Dynamics Division, National Center for Atmospheric Research, P.O. Box 3000, Boulder, CO 80307-3000, USA. (jenkay@ucar.edu)